Load carrying capacity of keyed joints reinforced with high strength wire rope loops

Jørgensen, Henrik B.; Hoang, Linh Cao

Published in:
Proceedings of fib Symposium 2015

Publication date:
2015

Document Version
Publisher's PDF, also known as Version of record

LOAD CARRYING CAPACITY OF KEYED JOINTS REINFORCED WITH HIGH STRENGTH WIRE ROPE LOOPS

Henrik B. Joergensen[1] and Linh C. Hoang[2]

[1]Department of Technology and Innovation, University of Southern Denmark
[2]Department of Civil Engineering, Technical University of Denmark

Abstract

Vertical shear connections between precast concrete wall elements are usually made as keyed joints reinforced with overlapping U-bars. The overlapping U-bars form a cylindrical core in which the locking bar is placed and the connection is subsequently grouted with mortar. A more construction friendly shear connection can be obtained by replacing the U-bars with high strength looped wire ropes. The wire ropes have the advantage of being flexible (they have virtually no bending stiffness) which makes installation of wall elements much easier. The looped wire ropes are usually pre-installed in so-called wire boxes which are embedded in the precast wall elements. Once the joint is grouted with mortar, the boxes will function as shear keys and the overlapping wire loops will function as transverse reinforcement that replaces the U-bars.

This paper presents a rigid-plastic upper bound model to determine the shear capacity of wire loop connections. Tests have shown that the shear capacity of such joints – due to the relatively high tensile strength of the wire ropes - is more prone to be governed by fracture of the joint mortar in combination with yielding of the locking bar. To model this type of failure, so-called multi-body mechanisms have to be considered. It is shown that calculations based on multi-body mechanisms lead to results that agree well with experiments.

Keywords: Plasticity modelling, precast concrete elements, shear connections, wire rope loops

1 Introduction

This paper deals with the in-plane shear capacity of vertical wire loop connections between precast concrete wall elements. The results presented are based on a PhD study recently completed by the 1st author (Joergensen, 2014).

Traditionally, connections between precast wall elements are made as keyed joints transversely reinforced with overlapping U-bars. The overlapping U-bars are normally placed pairwise with contact and form a cylindrical core, which confines a so-called lock bar. In building structures, such shear connections are usually grouted with mortar. In practice, the assembly sequence of the precast elements may require that a number of wall elements have to be installed (i.e. put in place) as a vertical “drop down”. This installation maneuver is only possible if the overlapping U-bars are bent up prior to installation. When the U-bars have diameter larger than about 10 - 12 mm, bend up and manual straightening of the U-bars after installation is not a practical option. In this context, the so-called wire loop connection (see e.g. Kintscher, 2007; Bachmann & Steinle, 2011) is a more construction-friendly solution. In wire loop connections, the U-bars are replaced by looped wire ropes. The wire ropes have the advantage of being flexible (they have virtually no bending stiffness) which makes vertical installation of the precast elements much easier. The wire loops are usually pre-installed in alumunium/steel boxes called wire boxes. The boxes contain either one or two pre-installed looped wire ropes (i.e. n_{wire} = 1 or 2) as illustrated in Fig. 1.

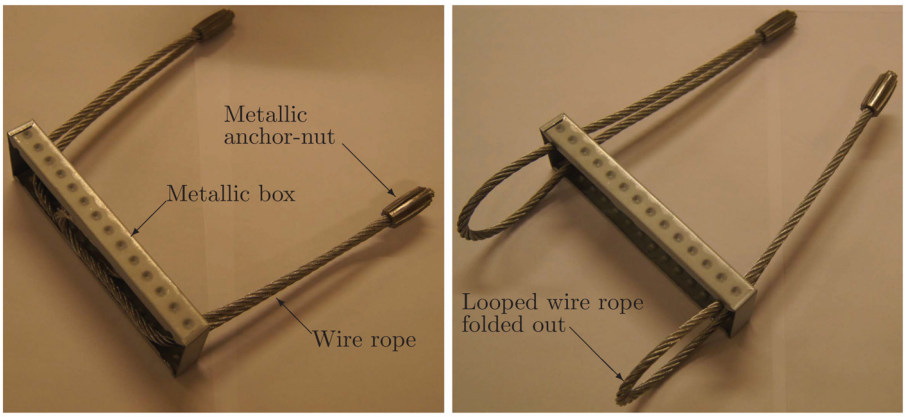

Fig. 1 Picture of a double wire box (a) before and (b) after the wires are folded out

Fig. 2 shows an example of how wire boxes are placed in a connection between two wall elements. The wire boxes have their opening facing the connection. Hence, when filled with mortar, the boxes will serve as shear keys.

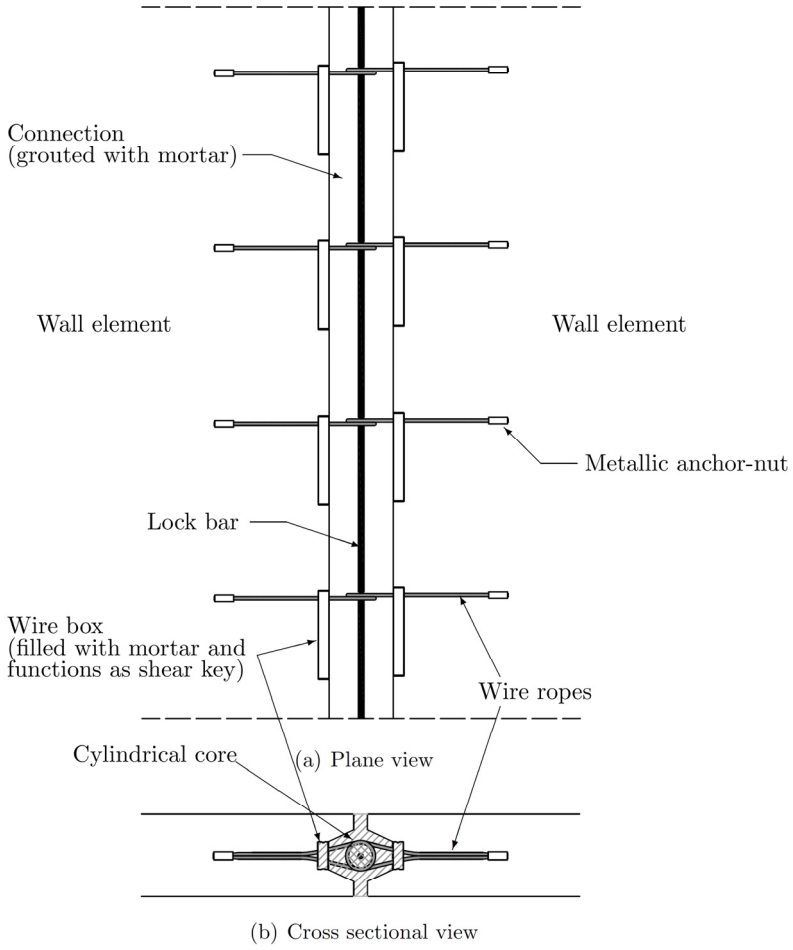

Fig. 2 Drawing of wire loop connection between two wall elements

The wire ropes that currently are available in the construction industry have a very brittle tensile failure without any yield plateau in the stress-strain relationship (Joergensen, 2014). As such, the wire ropes do not fulfil the code requirements to ductility (see e.g. Eurocode 2, 2005). These requirements are partly related to the use of plasticity design methods. To overcome the problem of brittle failure and to allow for stress redistributions, loop connections should be designed in such a way, that the

wire ropes become the “strongest link” in the connection. The load carrying capacity will in this way be governed by yielding of the lock bar in combination with crushing of the joint mortar. This design approach will ensure a warned failure, especially if the mortar is confined.

In the following theoretical treatment, the wire ropes are required to be the “strongest link”. Rigid-plastic upper bound solutions for the shear capacity of wire loop connections will be presented. The solutions are compared with test results. It is shown that good agreements between tests and theory can be obtained. In addition to the shear strength solutions, the paper also contains formulations of the design criteria, which will prevent failure of the wire ropes at the ultimate limit state.

2 Mechanism analysis and analytical solutions

In this Section, a rigid plastic upper bound model for calculation of the shear strength of wire loop connections will be presented. The failure mechanisms to be considered are idealisations and simplifications of the failures observed in tests.

The lack of ductility in the wire ropes means that plasticity modelling should not be carried out unless the wire ropes are the “strongest link” in the connections. In other words, the capacity of the connection has to be governed by failure in the mortar and/or yielding of the lock bar. This mode of failure will therefore be assumed and required in the following.

2.1 Tensile capacity of overlapping wire ropes

To transfer shear across the connection, the wire ropes have to be stressed to tension. Therefore, as a first step toward the calculation of the shear strength of the connections, there is a need to calculate the tensile capacity of the overlapping wire loops.

Wire ropes that are used in shear connections typically have a high tensile strength (larger than 1000 MPa) and a relatively small nominal cross sectional diameter, ϕ_w (typically 6 mm). The ropes are bend in a loop that typically has a diameter, D, in the order of 45-65 mm. The combination of these characteristics will in practice result in very high concentrated stresses in the parts of the joint mortar that are confined by the overlapping wire loops. The tension force that can be transferred between the overlapping loops may therefore be limited by local crushing of the joint mortar. One may imagine that the wire loops cut through the mortar. Such a failure mode is by no mean simple to model. In the following, the tensile capacity of overlapping wire loops will therefore be modelled in an approximate manner by assuming simplified stress states.

Fig. 3 shows an idealisation of two overlapping wire loops that transfer the tension force F_{wire}. The overlapping wire loops are assumed to form a circle with diameter corresponding to the loop diameter D. Since ϕ_w is significantly smaller than D, it may, as a start, be assumed that the loops confine a plane circular disc of mortar with diameter D and thickness ϕ_w. Due to F_{wire}, a plane hydrostatic compressive stress, σ_c, will develop in the disc. The following relation may be established:

$$\sigma_c \simeq \frac{F_{wire}}{D\phi_w} \tag{1}$$

In the direction of the lock bar, i.e. perpendicular to the plane of the circular disc of mortar, a confinement stress, $\sigma_{con} < \sigma_c$, is assumed to develop (see Fig. 3). The confinement stress is provided by the lock bar and can on the basis of lower bound plasticity reasoning be determined as follows:

$$\sigma_{con} = \frac{A_{sL} f_{yL}}{A_c} \tag{2}$$

Where A_{sL} and f_{yL} are, respectively, the cross sectional area and the yield stress of the lock bar while $A_c = 0.25\pi D^2$ is the area of the disc.

Strictly speaking, the above approximation of a circular disc with thickness ϕ_w requires the two wire loops to be placed at exactly the same level. This, of course, is not possible. An additional stress condition must therefore be considered. Since the wire loops are placed at different levels (but assumed to be in contact), shear stresses will have to develop in order to transfer F_{wire}. This is illustrated in Fig. 4. From equilibrium requirements, the shear stress, τ_c, can be determined as follows:

$$\tau_c = \frac{F_{wire}}{A_c} \tag{3}$$

where A_c, as mentioned, is the area of the confined disc.

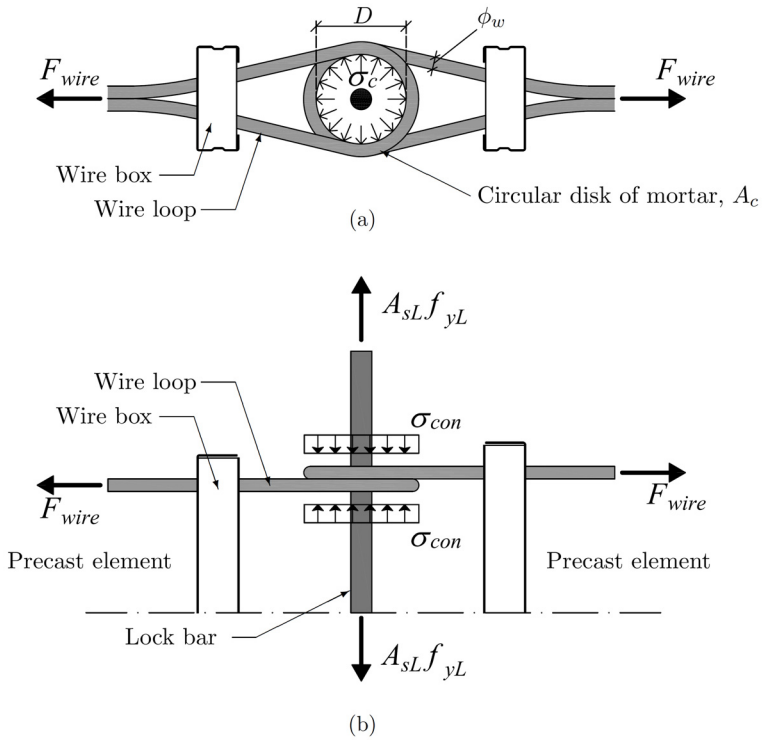

Fig. 3 Idealised stress state in circular disc of mortar within the overlap of wire loop; top view (a) and side view (b).

To establish strength criteria for σ_c and τ_c, a failure criterion for mortar in triaxial stress states is required. According to Nielsen and Hoang (2011), confined mortar behaves somewhat between concrete and cement paste. Therefore, in the following, a combination of the failure criterion for concrete and the failure criterion for cement paste will be adopted for confined mortar. The idea is simply to take the lower envelop curve of the two basis criteria. This should provide a lower bound to the failure criterion for mortar.

The modified Coulomb failure criterion usually adopted for concrete stressed in compression may be written as:

$$\sigma_c = f_c + k\sigma_{con} \quad (k = 4 \text{ for concrete}) \tag{4}$$

where k is equal to:

$$k = \frac{1+\sin\varphi}{1-\sin\varphi} \tag{5}$$

For normal strength concrete, the internal angle of friction may be taken as φ = Arctan(3/4), meaning that k = 4.

According to tests by Dahl (1992) and Hansen (1994), cement paste under tri-axial stress conditions with high confinement will behave like a material with frictional angle $\varphi = 0$, i.e. no dilatation takes place at failure and $k = 1$. Based on these tests, the failure criterion for highly confined cement paste may be written as (see also Nielsen & Hoang, 2011):

$$\sigma_c = f_{cc} + k\sigma_{con} \qquad (k = 1 \text{ for cement paste with } \varphi = 0) \tag{6}$$

Here f_{cc} is called the *apparent* uniaxial compressive strength which is greater than the *true* uniaxial strength f_c. The relationship between f_{cc} and f_c for cement paste can be obtained from tests. In this context, the results shown in Fig. 5 may be used. A more detailed discussion may be found in Joergensen (2014).

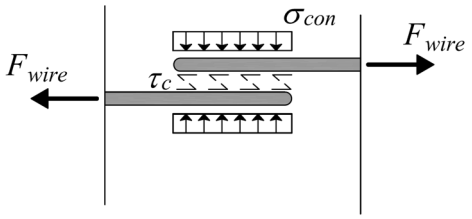

Fig. 4 Transfer of shear stress τ_c between overlapping wire loops

By combining criteria (4) and (6), the following lower envelop curve is obtained for calculation of the compressive stress that can be resisted by the disc of mortar confined by the overlapping wire loops:

$$\sigma_c = \min\begin{cases} f_c + 4\sigma_{con} \\ f_{cc} + \sigma_{con} \end{cases} \tag{7}$$

This criterion may be transformed into a (σ, τ)-stress space. When doing so, the following condition is obtained:

$$\tau = \min\begin{cases} \dfrac{1}{4} f_c + \dfrac{3}{4}\sigma_{con} \\ \dfrac{1}{2} f_{cc} \end{cases} \tag{8}$$

Now, with the strength and stresses defined, the tensile capacity of overlapping wire loops, F_{wire}, may be determined by combining Eq. (1) and (2) with Eq. (7) and Eq. (3) with Eq. (8). The result appears as follows:

$$F_{wire} = \min\begin{cases} \left(f_c + 4\sigma_{con}\right) D\phi_w & (a) \\ \left(f_{cc} + \sigma_{con}\right) D\phi_w & (b) \\ \left(\dfrac{1}{4} f_c + \dfrac{3}{4}\sigma_{con}\right) A_c & (c) \\ \dfrac{1}{2} f_{cc} A_c & (d) \end{cases} \tag{9}$$

On the basis of Eq. (9), it is now possible to estimate the plastic energy that is dissipated, when the overlapping wire loops are tensioned to F_{wire}. How this is done will be described in the next Subsection.

As mentioned, plastic modelling should not be carried out if rupture of the wire ropes is decisive. For this reason, the following requirement must be fulfilled:

$$F_{wire} < F_{wire,u} \sim f_{uw} A_{sw} \tag{10}$$

Here, $F_{wire,u}$ is the rupture strength of a wire loop (f_{uw} and A_{sw} being the tensile strength and the cross sectional area of the wire ropes, respectively). The condition stated in Eq. (10) leads to requirements to the mortar strength. As shown in Joergensen (2014), for the typical values of D, ϕ_w, A_{sL} and f_{yL}, rupture of wire ropes can be avoided if the joint mortar has a uniaxial compressive strength less than approximately 60 MPa.

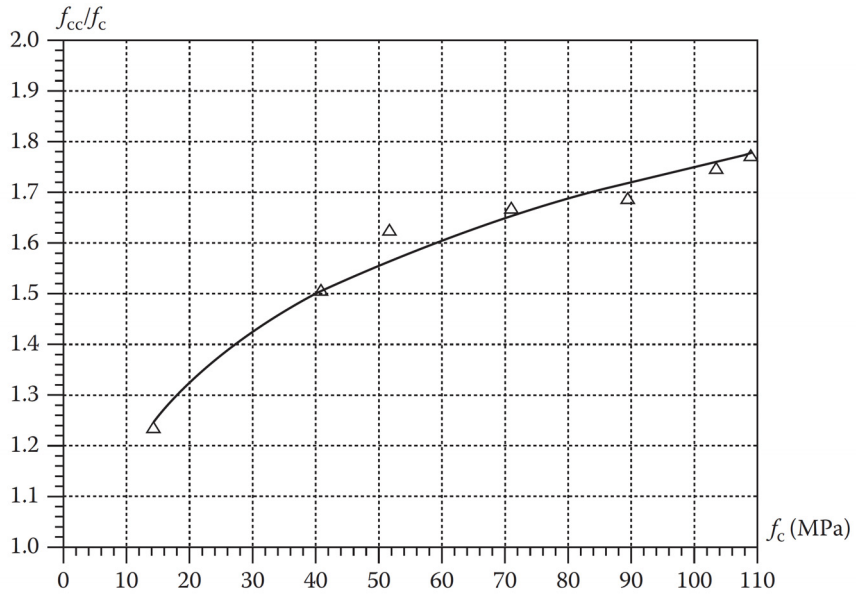

Fig. 5 Relationship between f_{cc}/f_c and f_c , from Nielsen & Hoang (2011)

2.2 Shear failure mechanism analysis

A number of tests conducted as push-off tests to study the shear strength of wire loop connections have been published (see Andersen & Poulsen, 2002; Frederiksen & Madsen, 2011; Hagsten, 2013). These tests show two typical failure modes, when the joint mortar is governing. In the following, these experimental observations will be used to develop and analyse two idealised shear failure mechanisms.

2.2.1 Mechanism without diagonal yield lines

The first type of mechanism involves only yield lines formed in the shear load direction. Fig. 6(a) shows the failure as observed in tests by Frederiksen & Madsen (2011). In the figure, the original positions of the wire boxes have been indicated as black lines. It appears from Fig. 6(a) that the relative displacement in the joint surfaces is practically the same over the entire length of the connection. This has been indicated by the red lines, which were drawn as continuous straight lines across the connection prior to testing. Based on this observation, an idealised failure mechanism is considered (see Fig. 6(b)). The mechanism, which is similar to one developed by Jensen (1976) for keyed shear joints, consists of vertical yield lines developed along the two joint surfaces. At the position of the wire boxes - which are filled with mortar - the yield lines have to cut through the mortar. Therefore, at these locations, plastic energy will be dissipated. The interface between the joint mortar and the precast elements is normally considered as smooth. Any resistance against failure at the smooth interfaces is neglected (In the tests considered in this paper, the interfaces were greased before casting of the joint mortar). As shown in Fig 6(b), the precast elements are assumed to move away from the connection by the displacement vectors (u_t, u_l) and ($-u_t$, $-u_l$), respectively. The rate of displacement, u_t/u_l, dictates the amount of plastic energy to be dissipated in the yield lines crossing the opening area of the wire boxes. Detailed calculations of the dissipated energy may be found in Joergensen (2014). The calculations are based on the so-called dissipation formulas which may be found in Nielsen & Hoang (2011).

Besides of the plastic energy dissipated in the yield lines, there is also a contribution from the overlapping wire loops. This is so because the precast elements have a transverse component, u_t, which means that the tensile capacity of the overlapping wire loops has to be mobilised. Hence, whenever a vertical yield line crosses a wire loop, the wire loop will contribute with an internal work amounting to $F_{wire} \cdot u_t$.

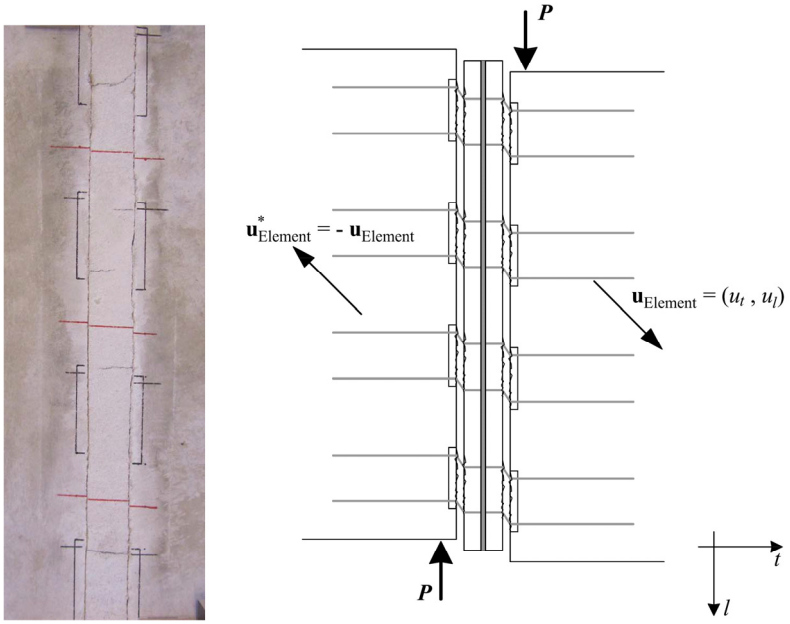

(a) (b)

Fig. 6 Failure mechanism without diagonal yield lines; (a) failure observed in tests by Frederiksen and Madsen (2011) and (b) idealised failure mechanism

By equating the total dissipated energy with the external work (in this case given as $2Pu_l$) an upper bound for the shear capacity of the connection may be found. This upper bound may then be minimised with respect to the rate of displacement, u_t/u_l, while keeping account of the normality condition of plastic theory. When doing so, an optimal solution is obtained. The solution reads (see Joergensen (2014) for further explanations):

$$P_{u,0} = \nu f_c n_{box} A_{box} \begin{cases} \sqrt{\frac{\Phi_T}{\nu}\left(1-\frac{\Phi_T}{\nu}\right)} & \text{for} \quad \frac{\Phi_T}{\nu} < \frac{1}{5} \quad \text{(a)} \\ \frac{1}{4}+\frac{3}{4}\frac{\Phi_T}{\nu} & \text{for} \quad \frac{\Phi_T}{\nu} \geq \frac{1}{5} \quad \text{(b)} \end{cases} \tag{11}$$

Here the subscript "u,0" indicates that the solution is related to a mechanism without diagonal yield lines. The factor ν denotes the effectiveness factor, which will be further discussed later. A_{box} denotes the opening area of each wire box and n_{box} is the number of wire boxes placed in one joint interface. Φ_T is the mechanical ratio of transverse reinforcement (the wire loops) and is given by:

$$\Phi_T = \frac{n_{wire} F_{wire}}{f_c A_{box}} \tag{12}$$

where n_{wire} denotes the number of wire loops pre-installed in each box (n_{wire} = 1 or 2).

2.2.2 Mechanism with diagonal yield lines

The second type of mechanism involves vertical as well as diagonal yield lines. Fig. 7(a) shows an example of this mechanism as observed in some tests by Frederiksen & Madsen (2011). It can be seen from the red lines drawn prior to testing that the relative displacement between the connection and the precast elements varies in the load direction. At the top, there is practically no relative displacement between the connection and the precast element on the left side, whereas a large relative displacement

is observed for the precast element to the right. At the bottom of the connection, the opposite scenario is observed. Finally, at the middle of the connection, the left as well as the right precast element is seen to have a relative displacement, which is about half of the displacement at the top and at the bottom. The observed failure has been idealised and simplified as shown in Fig. 7(b). Here, the system of vertical and diagonal yield lines divide the connection into a number of segments (three in the case shown). The centre segment has the shape of a parallelogram. The top segment of the connection is attached to the precast element on the left side and the bottom segment of the connection is attached to the precast element on the right side. When more than two boxes are placed in each precast element, the number of parallelogram shaped segments will increase. As an example, Fig. 8 shows the system of yield lines in a connection with four boxes in each precast element.

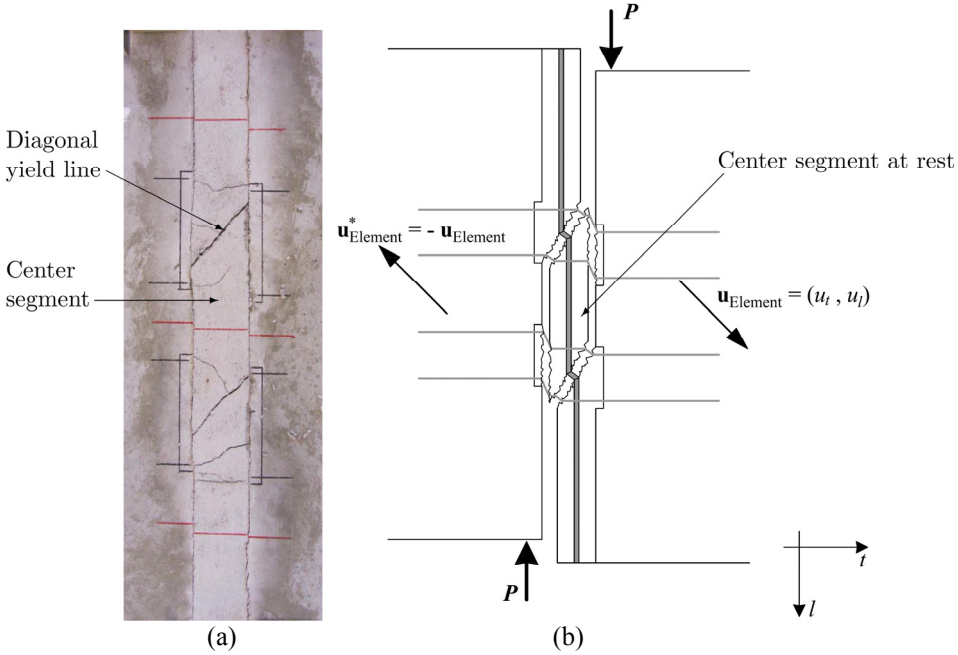

Fig. 7 Failure mechanism with diagonal yield lines; (a) failure observed in tests by Frederiksen and Madsen (2011) and (b) idealised failure mechanism

Similar to the case treated in Subsection 2.2.1, the rigid body displacements of the two precast elements are here described by the vectors (u_t, u_l) and ($-u_t$, $-u_l$), respectively. To obtain a variation in the relative displacements as observed in Fig. 7(a), the segments of mortar have to undergo rigid body displacement as well. With reference to Fig. 8, the centre segment is here assumed to be at rest while the two neighbouring segments are displaced by the vectors $\mathbf{u}_4 = (0, 2/4u_l)$ and $\mathbf{u}^*_4 = (0, -2/4u_l)$, respectively. The remaining two segments are attached to the precast elements and will therefore follow the same displacement as the respective precast element. From the described displacement field, it appears that the *relative displacement* in each of the diagonal yield lines is identical and amounts to $(0, 1/2u_l)$. This applies to the case shown in Fig. 8, while for the general case with n_{box} number of wire boxes, the relative displacement may be shown to be $(0, 2u_l)/n_{box}$ (Joergensen 2014). Finally, for each of the vertical yield lines, the relative displacement must be determined by subtracting the displacement vector of the adjacent segment of mortar from the displacement vector of the precast element. This results in different relative displacements depending on the position of the vertical yield lines. This has been illustrated in Fig. 8 by the vectors $\mathbf{u}_1$, $\mathbf{u}_2$, $\mathbf{u}_3$, $\mathbf{u}^*_1$, $\mathbf{u}^*_2$ and $\mathbf{u}^*_3$. The length and the direction of the vectors of relative displacement as described above are used to calculate the energy dissipated in the yield lines.

The diagonal yield lines are crossing the lock bar. Hence, in this mechanism, the lock bar has a direct contribution to the internal work (which at each diagonal yield line will be equal to the yield force of the lock bar multiplied by $2u_l/n_{box}$). Because the lock bar hereby is included directly, its yield capacity cannot once more be mobilised to develop confinement stresses in the circular core of mortar enclosed by the overlapping wire loops. This means that when the tensile capacity of the transverse

reinforcement (the wire loops) is determined, the confinement stress, σ_{con}, must be taken as zero. The tensile capacity, given in Eq. (9), is hereby reduced to:

$$F_{wire,0} = \min \begin{cases} f_c D \phi_w & (a) \\ \frac{1}{4} f_c A_c & (b) \end{cases} \tag{13}$$

Here, the subscripted "0" indicates that the tensile capacity is calculated with zero confinement stress. Eq. (13) is used when the contribution to the dissipated energy from the overlapping wire loops has to be calculated. This contribution amounts to $F_{wire,0} \cdot u_t$ whenever a vertical yield line crosses a wire loop. Now, by equating the total internal work with the external work, one will arrive at an upper bound for the shear strength associated with the considered failure mechanism. To enable presentation of the solution in a dimensionless form, it is convenient to introduce the parameter $\Phi_{T,0}$:

$$\Phi_{T,0} = \frac{n_{wire} F_{wire,0}}{f_c A_{box}} \tag{14}$$

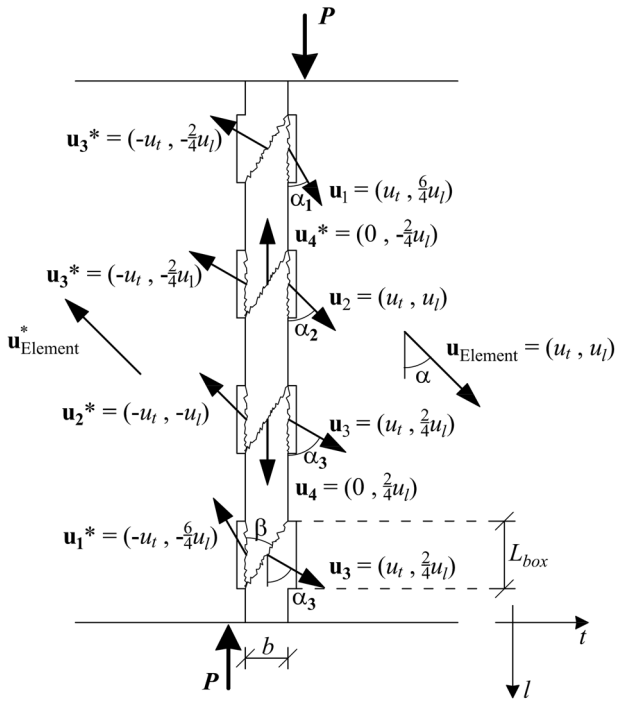

Fig. 8 Failure mechanism with diagonal yield lines and relative displacement vectors in yield lines

The upper bound solution for a connection with n_{box} number of wire boxes in each precast element may be shown to be (Joergensen 2014):

$$\begin{aligned} \frac{P_{u,1}}{\nu f_c n_{box} A_{box}} = {} & \frac{\tan\alpha}{n_{box}} \sum_{i}^{n_{box}-1} \frac{\frac{1}{2}}{\sin\left(\arctan\left(\frac{n_{box}}{2(n_{box}-1)}\right)\tan\alpha\right)} \\ & + \tan\alpha \left[\frac{\frac{A_d}{n_{box} A_{box}}}{2\sin\left(\arctan\left(\frac{n_{box}}{2}\tan\alpha\right)\right)} + \frac{A_{box} - t L_{box}}{2 n_{box} A_{box}} + \left(\frac{\Phi_{T,0}}{\nu} - \frac{1}{2}\right) \right] \\ & + \left(\frac{\Phi_L}{\nu} - \frac{1}{2}\right) \frac{bt}{n_{box} A_{box}} + \frac{n_{box} - 2}{2 n_{box}} \frac{A_d}{n_{box} A_{box}} \end{aligned} \tag{15}$$

In solution (15), b and t denote, respectively, the width and depth of the connection and L_{box} is the length of the wire box (in the shear load direction). A_d is the surface area of a diagonal yield line and Φ_L defines the mechanical ratio of the lock bar:

$$A_d = t\sqrt{b^2 + {L_{box}}^2} \tag{16}$$

$$\Phi_L = \frac{f_{yL} A_{sL}}{f_c bt} \tag{17}$$

The upper bound solution (15) is seen to be a function of the displacement rate: $\tan\alpha = u_t/u_l$. An optimal upper bound solution may therefore be found by minimisation with respect to $\tan\alpha$. Unlike the previous case, it is here not possible to determine an analytical optimal solution. The result has to be found numerically. In this context, it is important to take into account the normality condition of plastic theory. This may be shown to imply, that $\tan\alpha$ must fulfil the following condition (see Joergensen, 2014):

$$\tan\alpha = \frac{u_t}{u_t} \geq \frac{3}{2}\frac{n_{box} - 1}{n_{box}} \tag{18}$$

2.3 Shear strength of wire loop connections

On the basis of the two failure mechanisms considered, the shear capacity of a wire loop connection should now be taken as the minimum of the optimised results, i.e.:

$$P_u = \min \begin{cases} P_{u,0} & \text{(Eq. (11))} \\ P_{u,1} & \text{(Eq. (15)) ; minimised with respect to } \alpha \end{cases} \tag{19}$$

Fig. 9 shows an example on how P_u varies with Φ_T/ν. The failure mechanism without diagonal yield lines appears to be decisive for low mechanical ratios of transverse reinforcement while the mechanism with diagonal yield lines is governing for high mechanical reinforcement degrees.

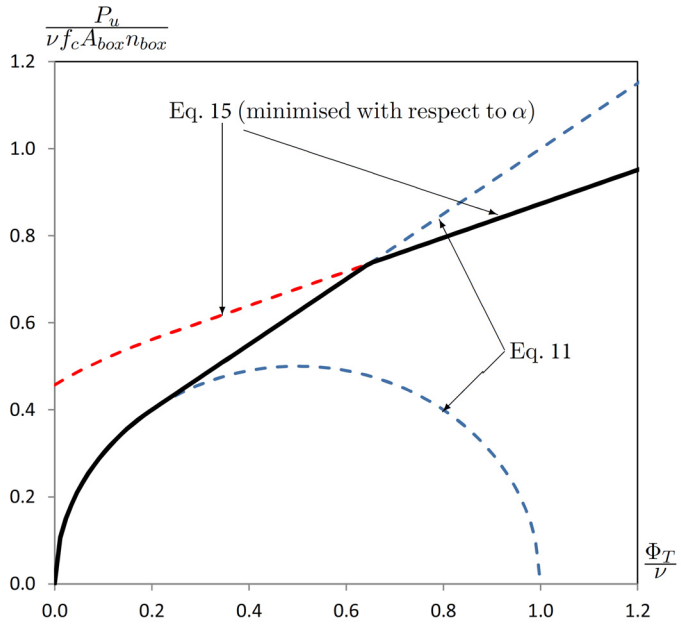

Fig. 9 Shear strength versus mechanical ratio of transverse reinforcement
(data used are; $n_{box} = 4$, $\Phi_T / \Phi_{T,0} = 2.89$, $A_d/A_{box} = 4.79$, $t/b_{box} = 4.29$, $bt/A_{box} = 2.14$, $\Phi_L = 0.26$, $\nu f_c = 15.8$ MPa)

3 Comparison with test results

As usual when applying the theory of plasticity to structural concrete it is necessary to introduce the so-called effectiveness factor ν. This factor takes into account the softening and cracking behaviour of concrete/mortar as well as other phenomena not included in the simplified plastic solutions. The effectiveness factor can either be found by calibrating the theoretical solution with test results or be adopted from a similar well-documented problem. In the present study, a combination of the two mentioned approach is used. Since the shear problem considered here bears resemblance to beam shear problems, it is worthwhile to investigate if the structure of a ν-formula for shear in beams can be used. Zhang (1994) developed the so-called Crack Sliding Model for calculation of the shear strength of beams without shear reinforcement and adopted the following basis formula:

$$\nu_{beam} = \frac{0.88}{\sqrt{f_c}}\left(1+\frac{1}{\sqrt{h}}\right)(1+26\rho) \qquad \left(f_c \text{ in MPa and } h \text{ in meters}\right) \tag{20}$$

Here, the height of the beam cross section h reflects a size effect associated with the size of the diagonal yield line in the shear load direction. The dependency on the ratio of longitudinal reinforcement, ρ, is mainly due to dowel action. In the case of a wire loop connection, the geometrical parameter that dictates the size of the yield lines in the direction of the shear load is L_{box}. Further, there is no dowel action in a wire loop connection loaded in shear because the wire ropes are flexible. Based on these qualitative arguments, the applicability of the following formula has been investigated.

$$\nu = \frac{K}{\sqrt{f_c}}\left(1+\frac{1}{\sqrt{L_{box}}}\right) \qquad \left(f_c \text{ in MPa and } L_{box} \text{ in meters}\right) \tag{21}$$

where K does not necessarily have to be 0.88 as in Eq. (20) because this equation applies to concrete while in the present problem, the connection is grouted with mortar. Since mortar has a smaller aggregate volume content than concrete and since the maximum aggregate size in mortar is normally 2-4 mm or less, then the effect of aggregate interlock can be expected to be less pronounced in diagonal yield lines formed in mortar than in concrete. Formula (21) has been incorporated in the theoretical solution (19) and compared with the available test results (see Andersen & Poulsen, 2002; Frederiksen & Madsen, 2011; Hagsten, 2013). It turns out that that by choosing K = 0.75, a mean value of 1.0 is obtained for the test to model ratio. The corresponding standard deviation amounts to 0.16 (see Joergensen 2014).

Fig. 10 shows a comparison between calculated and tested shear capacity. In the figure, red coloured marks correspond to tests where the mechanism with diagonal yield lines was critical according to calculations. In addition, circular marks denote tests with single wire boxes (i.e. $n_{wire} = 1$) whereas square marks denote tests with double wire boxes (i.e. $n_{wire} = 2$).

The tests calculated to fail without development of diagonal yield lines have been collected in Fig. 11. In this plot, the dependency of P_u on the transverse reinforcement degree Φ_T is clearly seen.

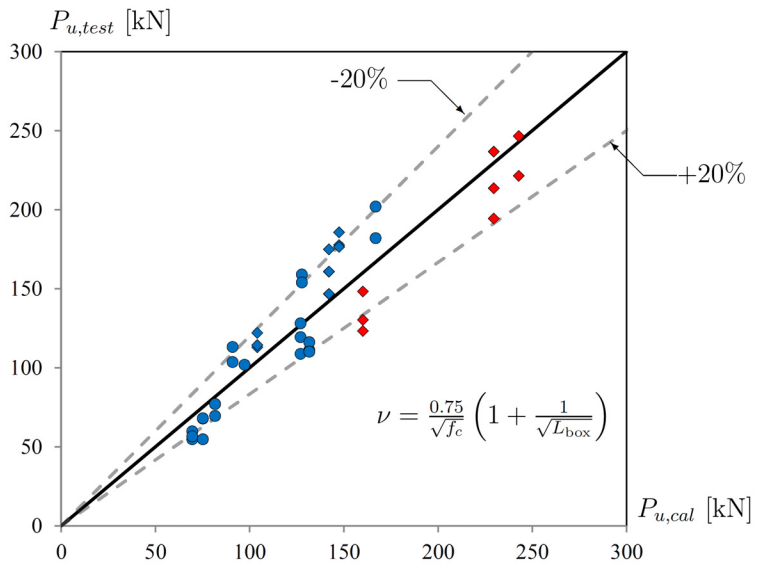

Fig. 10 Comparison of calculated shear capacity, $P_{u,cal}$, and tested shear capacity, $P_{u,test}$.

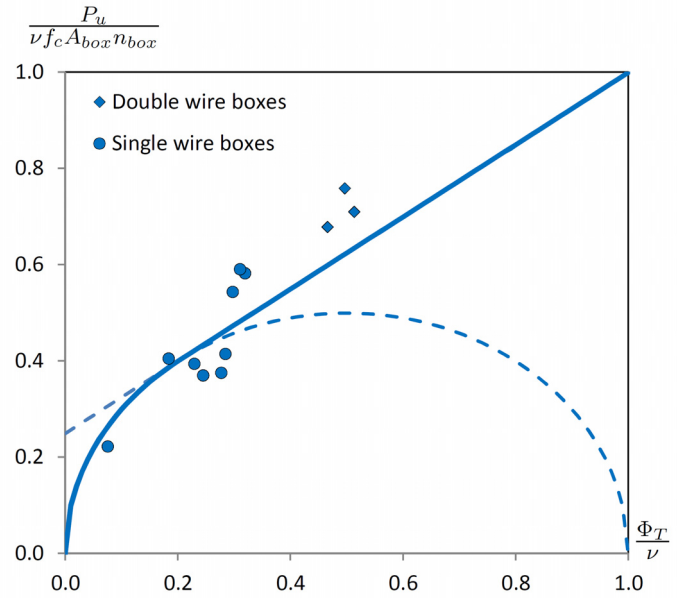

Fig. 11 Comparison of model with test results for specimens predicted to fail without development of diagonal yield lines.

4 Conclusions

Experimentally observed failure mechanisms have been used as inspiration to develop upper bound plastic solutions for the in-plane shear capacity of wire loop connections. Two different failure modes were treated. In the first mode (failure mode 1), yield lines only develop along the joint surfaces and cutting through the opening areas of the mortar filled wire boxes. In the second mode (failure mode 2), diagonal yield lines also develop, running across the connection from one edge of a wire box to the opposite edge of the adjacent box.

In order to apply the presented plastic solutions, it is required that rupture does not take place in the wire ropes due to their brittle behavior in uniaxial tension. In this context, a simple model for the tensile capacity of pairs of overlapping wire loop has been developed for the case where crushing of the confined mortar is governing. The model is based on a combination of the failure criteria for concrete and for cement paste and enables the designer to choose a design, where rupture of wire ropes

can be avoided. The results of the tensile capacity model have been used in the calculations of the internal plastic work associated with the shear failure.

The shear strength model predicts failure mode 1 when the mechanical degree of transverse reinforcement (i.e. wire loops) is low. For higher degree of transverse reinforcement, failure mode 2 is critical. The model has been compared with tested shear strength. It is shown that good agreement can be achieved by adopting a modified version of a formula for the effectiveness factor originally proposed for beam shear problems.

References

Andersen, H.B. and Poulsen, D. G. (2002), Liner i præfabrikerede betonelementer (Translated: Wires in precast concrete elements). Master's thesis, Department of Civil Engineering, Technical University of Denmark, Denmark. (In Danish).

Bachmann, H. and Steinle, A. (2011), Precast Concrete Structures. Ernst and Sohn GmbH & Co. KG., first edition.

Dahl, K. K. B. (1992), A failure criterion for normal and high strength concrete. Technical report, Department of Structural Engineering, Technical University of Denmark. Report No. R-286.

Eurocode 2 (2005), Eurocode 2: Design of Concrete Structures – Part 1-1: General rules for buildings. Danish Standards, second edition. DS/EN 1992-1-1.

Frederiksen, M. S. and Madsen, K. (2011), Elementsamlinger med wirebokse – eksperimentel undersøgelse af forskydningsstyrker og deformationsegenskaber (Translated; Precast element connections with wire boxes – Experimental study on shear and deformation properties). Master's thesis, Architectural Engineering, Aarhus School of Engineering, Denmark. (In Danish).

Hagsten, L. G. (2013), Element connection with Pfeifer wireboxes. Technical report, Aarhus University School of Engineering, Denmark.

Hansen, T. C. (1994), Triaxial tests with concrete and cement paste. Technical report, Department of Structural Engineering, Technical University of Denmark, Denmark. Report No. R-319.

Jensen, B. C. (1976), Nogle plasticitetsteoretiske beregninger af beton og jernbeton. PhD thesis, Institute of Building Design, Technical University of Denmark. English translation published in 1977: Jensen, B. C. (1977), Some applications of plastic analysis to plain and reinforced concrete, Report No. 123.

Joergensen, H.B. (2014), Strength of loop connections between Precast Concrete Element – Part 1: U-bar connections loaded in combined tension and bending – Part 2: Wire loop connections loaded in shear. Ph.D. thesis, University of Southern Denmark, Denmark.

Kintscher, M. R. (2007), The VS ®system – A success story achieved through consistent further development. BFT International, (8):26-39.

Nielsen, M. P. and Hoang, L. C. (2011), Limit Analysis and Concrete Plasticity. CRC Press, third edition.

Zhang, J. P. (1994), Strength of Cracked Concrete, Part 1 – Shear Strength of Conventional Reinforced Concrete Beams, Deep Beams, Corbels and Prestressed Reinforced Concrete Beams Without Shear Reinforcement. PhD thesis, Department of Structural Engineering and Materials, Technical University of Denmark, Denmark. Report No. R-311.